

Creation of sealed strong structures of rocket and space equipment FDM printing methods by ULTEM™ 9085 PEI plastic

A.F. Salenko¹ • I.I. Derevianko² • A.A. Samusenko² • K.V. Avramov³ • A.V. Lithot² • V.V. Rogulin²

Received: 9 August 2021 / Accepted: 24 November 2021

Abstract. The work shows the possibility of manufacturing products for rocket and space technology using the additive FDM-printing technology. The object of research is the nozzle plugs of the “membrane” type. Considering the specific-strength properties of the product during its operation during operation, as well as the features of the FDM-process, the design was optimized, the regularities of the formation of its properties were established. An impregnation technology has been developed to seal the product. The equipment was designed, and pneumatic tests were carried out. The properties of materials were investigated considering their guaranteed shelf life for 12 years of operation under accelerated climatic tests. It is shown that the production of products by FDM-printing methods is promising and expedient, since the properties being formed are predictable, achievable, and stable.

Keywords: nozzle plug, additive technologies, 3D printing, strength calculations, pneumatic tests.

Introduction

Non-metallic materials used in the rocket and space industry is a compromise between low weight, high physical and mechanical properties, and safety. The operation of lightweight structures made of these materials must meet the following parameters [1, 2]:

- minimum weight;
- maximum rigidity and strength of parts;
- maximum service life of structures under operating conditions;
- high reliability.

Recently, in addition to increasing the specific-strength and resource properties of materials and structures, the issue of increasing costs for the manufacture and development of products in a single production is acutely felt. The introduction of 3D printing technology (in particular, FDM processes), which makes it possible to manufacture products of any shape and complexity in one technological transition, without additional processing, is seen as

an alternative to expensive shaping tooling for the manufacture of complex-shaped products with subsequent machining. Despite the obvious advantages of the technology, the use of such materials in the structures of rocket and space technology (RST) has not been introduced due to several features, in particular, limited strength properties, the resulting anisotropy determined by the printing (layout) conditions, the permeability of the resulting products to gases, and in some cases, highly fluid liquids, low temperature resistance, and others.

Thus, the possibility of obtaining reliable sealed products of a given strength, capable of retaining the properties of properties for a long time, is the main condition for the application of these processes in the manufacture of aerospace vehicles [3].

Possibilities of the method

The scheme of laying layers of material for any printers and modifications of manipulation systems remains layered, with the reproduction of a given model from a flat platform. In this case, the model (product) A is conditionally intersected by many surfaces s_i parallel to the desktop XOY , each of which is separated from the other by a step δ_z , which is determined by the nozzle used (diameter d_s , filament diameter D_f , teaching speed v_s and other factors (Fig. 1).

✉ A.F. Salenko
salenko2006@ukr.net

¹ Igor Sikorsky Kyiv Polytechnic Institute, Kyiv, Ukraine;

² Yuzhnoye State Design Office;

³ A.N. Podgorny Institute of Mechanical Engineering Problems NAS of Ukraine.

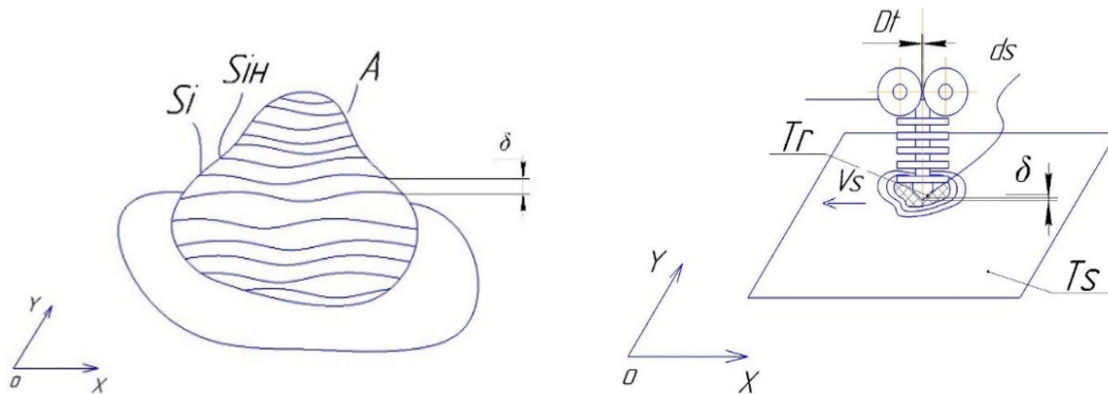


Fig. 1. Scheme of product formation *A* FDM-printing

Due to this layering, a set of indicators of the finished product is formed its accuracy (reproduced in the main ords, $\Delta_x, \Delta_y, \Delta_z$ strength $\sigma_x, \sigma_y, \sigma_z$, etc.).

At the same time, several researchers who paid attention exclusively to the accuracy of shape reproduction [4, 5], surface quality [6], as well as deformability of finished products after the process [7], noted that these parameters are due to both extrusion modes and the scheme of teaching the polymer melt. The same applies to another important issue - the question of the strength of products, the possibility of using printed parts in structures and mechanisms [8]. We have already noted in [9] that the use of printed elements in working structures requires additional solutions to the accuracy of printing (ensuring the quality of *IT* dimensions, the relative position of surfaces ($IT/2$), accuracy of form ($IT/2 \dots IT/3$) surface roughness (R_z, R_a), ensuring the strength of the extruded material σ_m and inter-layer strength σ_a .

The authors [9] showed that during the FDM process with PEEK plastic the surface morphology is directly affected by the melt pressure T_r due to the filament feed rate v_f and the extrusion diameter d_e , and the number of surface defects decreases with increasing melt pressure. However, the fluctuating extrusion force is the main limitation of the stability of the extrusion process.

The maximum filament compression force T_r determines the maximum extrusion speed, and the minimum extrusion force is the main determinant of slippage. Below the extrusion speed of 109.8 mm/min, the extrusion characteristic is in a relatively stable state. In this situation, the fiber with a diameter of D_f can provide an extrusion force to maintain the flow of the melt stably and continuously. During extrusion, a change in the size of the heated nozzle was observed, which was found to correlate with the instability of the PEEK filament size. There is a good linear relationship between the extrusion speed and the diameter of the extrusion filament in the range of extrusion speeds of $5 \text{ mm/min} < V_e < 80 \text{ mm/min}$. This is generally well correlated with the results obtained in [10].

Experiments have confirmed that the angle of application and the thickness of the layer δ , have a significant

effect on the strength and elongation at tensile, compressive and three-point bending. Optimal mechanical properties of PEEK or PEI were found in samples with a layer thickness of 300 μm and a teaching angle of $0 \dots \pi/2$. The mechanical properties of PEEK and ABS samples were compared. It was concluded that the strength characteristics of the investigated parts are lower for products obtained by 3D printing, compared with the same samples, but created from raw materials thermoplastic machines.

It is noted that the strength of a printed PEEK sample is about 45...56 MPa, which is equivalent to the strength of nylon parts during injection molding. Other hands the mechanical properties of printed samples with PEEK (in tension, compression and bending) were higher than those of ABS samples printed by commercial 3D printers by 108 %, 114 % and 115 %, respectively, with almost no significant difference. between the compression and bending module PEEK and ABS.

In [12] the results of research of influence of orientation of teaching of fibers on quality of a surface are resulted the geometrical model for definition of the profiles of roughness received with various angles of orientation of the press in FDM processes is presented. The surface quality was monitored by the average height of the roughness profile (parameter R_a).

The following conclusions authors formulated:

1) at small angles of orientation of the press regular profiles in which peak amplitude corresponds to height of a layer turn out. At large print orientation angles, the peak width increases, forming a flat area or gap between successive peaks;

2) the effect of stepwise steps is a general trend inherent in both the simulated and experimental values of the amplitude roughness. The step increases with increasing angle of the print, and reaching the value of $\pi/3$, the step begins to decrease;

3) depending on the angles of teaching and changes the shape of the profile curve.

Assuming the difference in the properties of printed samples due to the weakening of the adhesive adhesion of the layers of material after hardening, some researchers

have studied the process of laying the layers and its effect on the mechanical properties of the product and printing accuracy. The most thorough work is [13], which allowed to obtain a few patterns based on the comparison of the processes of layering in FDM printing for ABS and PLA plastics.

The main conclusion is the anisotropy of the properties of products that are in some way oriented relative to the main types of the printer, i.e. $[\sigma_x] \neq [\sigma_y] \neq [\sigma_z]$; $[\sigma_i] = f(i, j, k)$.

The PEEK curve is significantly different from the ABS curve. With increasing load, the peak first occurs at maximum stress, then a crack appears on the surface and there is a deformation of the neck, which ends in destruction at a time when the deformation reaches 87%. In PEEK or PEI samples there is no obvious deformation of the neck; there are also no cracks until the deformation of the sample and its destruction. However, for both ABS and PEEK, PEI, the strength was 0.5...0.6 $[\sigma]$ of filament.

However, most researchers believe that the mechanical properties of 3D-printed parts PEEK can be improved in the future by improving the accuracy of temperature control and hardware accuracy of the 3D-printing system. Need to say that the $[\sigma_i] = 70...95$ MPa is characterizing only the high temperature plastic such as PEEK or PEI.

Thus, the analysis of existing developments proves that the shape of the product, the method of its cultivation directly determines the strength characteristics, which, along with the orientation relative to the movement of the print head and temperature regimes, must be rationally provided in the FDM process.

At the same time, the question of the density of the extruded filament and the strength of the adhesive bond planes has been insufficiently studied by scientists. There is also no systematic information on changes in the properties of printed products over time, including in operating conditions

Formulation of the problem

Previously, experience was gained in the manufacture of FDM elements of technological equipment used in the production of individual elements of rocket and space technology. The main requirements for such elements were:

- 1) the accuracy of the form,
- 2) stability under working load,
- 3) endurance to elevated temperatures.

These objects were quite simple in shape, and the results of tests and metrological verification are covered in [11].

Some examples of parts printed on FDM printers are shown in fig. 2. Their feature is a high accuracy of the dimensions, shape accuracy, as well as the stability of the properties and parameters of the surface layers.

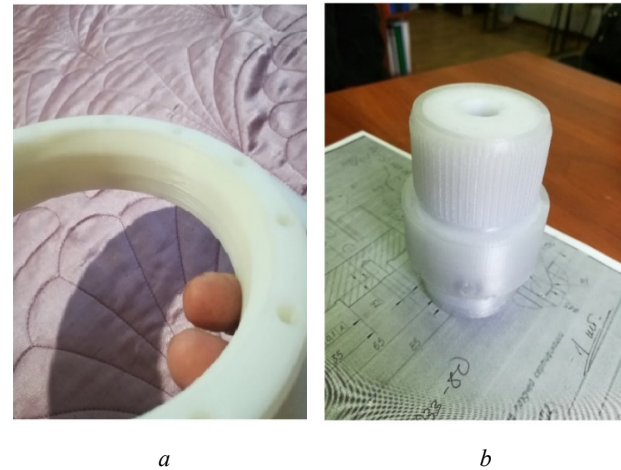


Fig. 2. Samples a parts, getting FDM printing: flange of chamber (a) and shafts (b)

A nozzle plug installed in the nozzle of a rocket engine was selected as an object of analysis now, Fig. 3.

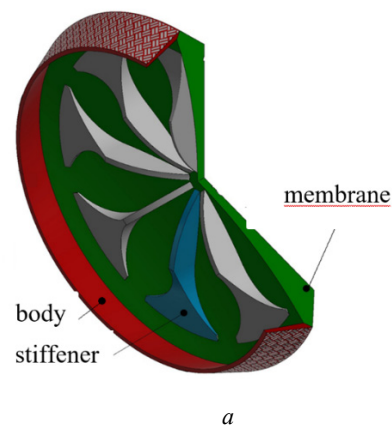


Fig. 3. Nozzle plug (a) and its installation into the nozzle of the main engine (b)

As usually, aluminum alloys are used as the nozzle plug material. The plug developed at the Yuzhnoye Design Bureau is completely made of thermoplastic and does not have metal inserts, while the use of such materials reduces its weight, which also minimizes the size of the danger zone for service personnel when it is triggered. In addition, hitting possible obstacles, such plugs are destroyed, while reducing the likelihood of damage to structural elements and personnel during a ricochet.

The developed nozzle plug is one integral part, which can be conditionally divided into 3 parts: body, fin and membrane. Each of them has its own functional purpose:

- opening zone – the joint between the body and the membrane, the strength of which should be minimal in the structure and at the same time ensure the operation of the plug in the range of gas-dynamic pressure ($0,6 \pm 0,3$) MPa;
- the body is made conical with a ribbed outer surface and is designed for tight and strong gluing directly to the nozzle material, the strength of the gluing, taking into account its area, should be higher than the strength of the opening zone;
- the membrane is made hermetic due to material impregnation and is designed to protect the inner space of the nozzle from external factors;
- stiffening ribs are designed to strengthen the membrane in such a way that the destruction of the nozzle plug is carried out not along the membrane itself, but along the opening zone.

The prototypes of the nozzle plug were presented in the following versions, Fig. 4.

The original version had a 3 mm thick membrane with an annular groove 1 mm deep to weaken the section (the supposed fracture site), 12 ribs converging in the center to concentrate the stresses acting on the membrane. The outer area of the body for the bonding is 224.3 cm², weight 212 g. The version of the nozzle plug, having a membrane thickness of 4–11 mm, had 8 ribs of a more complex configuration for even distribution of stresses acting on the membrane. The outer area of the body for the gluing has decreased to 205.1 cm² due to the decrease in the body height. Mass due to massive ribs increased to 298 g. The final version of the nozzle plug had a smoothly varying membrane thickness from 4 mm to 14 mm, 8 ribs for uniform distribution of stresses acting on the membrane. The outer area of the body for the gluing has decreased to 108.8 cm² due to the decrease in the body height. Due to the increase in membrane thickness, the mass increased slightly, up to 317 g. The summary parameters of all variants of nozzle plugs in table 1 are given.

Preliminary analysis of designs of nozzle plugs of variants performed using CAD software Autodesk Inventor Professional 2018. For each analysis the following conditions are accepted: the material of the part is isotropic; the load is applied to the surface from the side of the working cavity; the outer surface of the body is rigidly fixed and has no movement; plastic deformations begin at stresses above 33 MPa; destruction begins at internal stresses over 42 MPa.

Table 1. Basic parameters of all variants of nozzle plugs

Option plugs	Quantity ribs, pcs.	Thickness membrane, mm	Weight, g	Area inserts, cm ²	Pressure area, cm ²
1	12	3	212	224,3	228,66
2	8	4–11	298	205,1	198,65
3	8	4–14	317	108,8	222,87

For option No. 1, (Fig. 4, a) the expected fracture pressure was 0.4 MPa; the maximum value of stresses is in the annular groove at the point of transition of the membrane into the body; the place of the beginning of the destruction is in the annular groove; stress concentration – at the center of the ribs; the maximum calculated displacement of the center of the membrane at a pressure of 0.15 MPa – more than 1.0 mm, at a pressure of 0.3 MPa – more than 3.0 mm. This option has a low response pressure and high displacement rates, which does not exclude the possibility of damage to the impregnation material, which ensures the tightness of the part, in the process of repeated loading with a certain cyclicity.

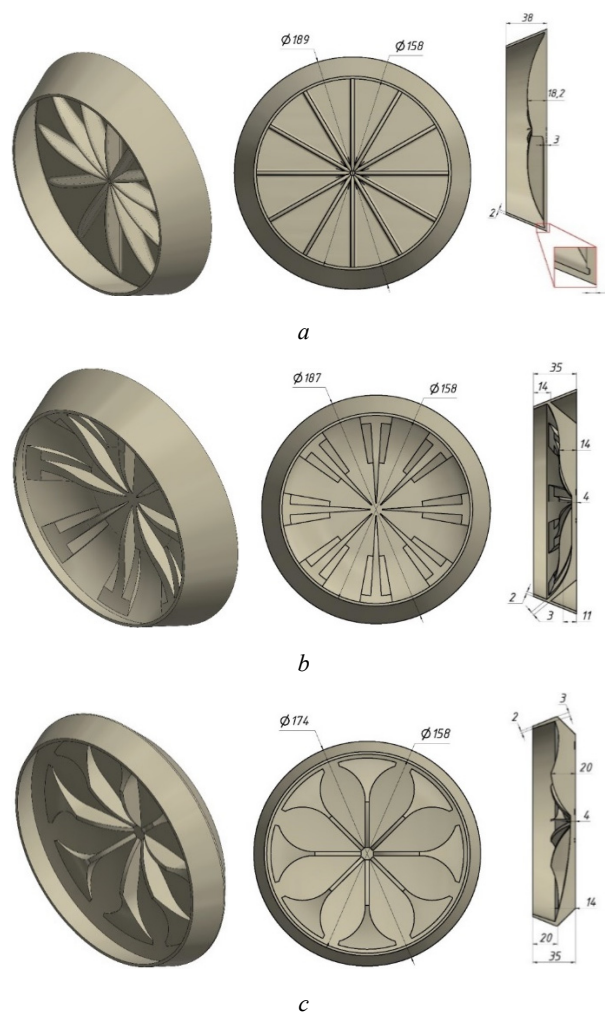


Fig. 4. Options of the nozzle plug: a) No. 1; b) No. 2; c) No. 3

Option No. 2 (Fig. 4, *b*) turned out to be more successful: the expected fracture pressure is 1.05 MPa; the maximum value of stresses is at the point of transition of the membrane into the body; the place of the beginning of destruction – along the line of transition of the membrane into the body; stress concentration – in places where ribs are present on the inner side of the body; the maximum calculated displacement of the center of the membrane at a pressure of 0.15 MPa is about 0.55 mm, at pressure of 0.3 MPa – more than 1.1 mm.

This option has a high response pressure, exceeding the working range requirement, but low displacement rates indicate a high structural rigidity. In the center, on the reverse side of the membrane, there is a stress concentration, while on the side of the working cavity, there is no stress concentration. These stresses are not critical and indicate the presence of displacements in the central region of the membrane.

The last option (Fig. 4, *c*) showed the following results: fracture pressure – 0.7 MPa; the maximum value of stresses is along the transition of the membrane to the body; the place of the beginning of destruction – at the point of transition of the membrane into the body; stress concentra-

tion – from the side of the working cavity along the circumference of the membrane transition into the body; the maximum calculated displacement of the center of the membrane at a pressure of 0.15 MPa – no more than 0.62 mm, at a pressure of 0.3 MPa – about 1.25 mm. This option has an optimal response pressure within the operating range. A slight increase in the movement of the membrane in comparison with option No. 2 is not critical. The stress concentration is dispersed along the edges of the membrane, which indicates the optimal shape of the ribs as elements of the load distribution acting on the membrane.

Thus, based on the strength calculations carried out in the CAD software Autodesk Inventor Professional 2018, the nozzle plug option No. 3 is the closest to the functional requirements (Fig. 5). It is this variant of the nozzle plug that is most expedient to choose as the main one. For it, additional strength calculations were carried out in the software of the Ansys Static Structural package to refine and compare the results. Strength calculation is carried out in order to determine the displacements when checking the plug for tightness, as well as to determine the response pressure of the plug.

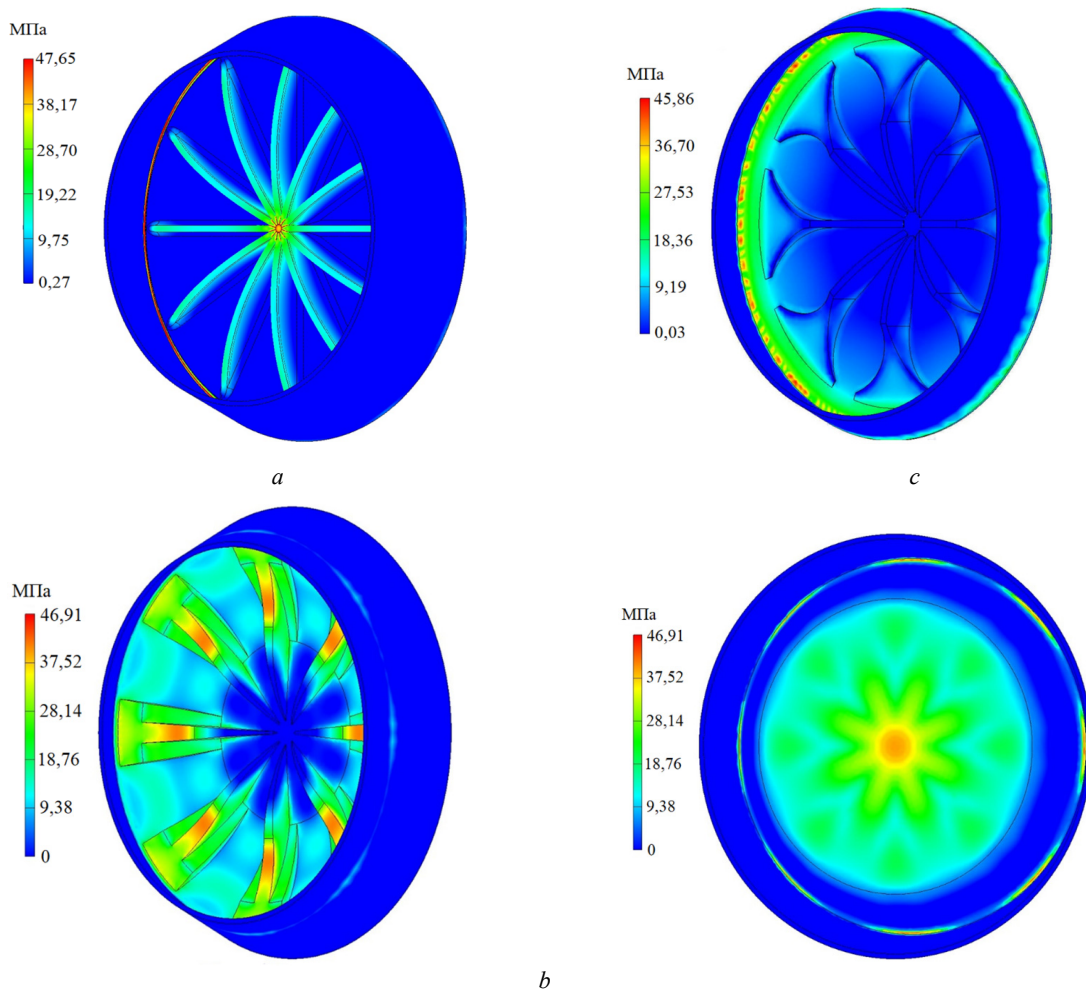


Fig. 5. Stress state of a product before failure (*a*) – No. 1; (*b*) – No. 2; (*c*) – No. 3

Development of the technology of gluing the nozzle plug into the nozzle block

Let us consider the different behavior of adhesive joints for different variants of the surface of the nozzle plug body. To glue the nozzle plug into the nozzle simulator, we used EPOTERM-03t type A epoxy glue, which is also used for impregnating the material. The thickness of the adhesive layer can vary from 0.1 mm to 0.5 mm.

The primary task is to select the height of the nozzle plug body, and, accordingly, its outer area, which corresponds to the area of the glue joint of the plug with the nozzle. The opening pressure of the plug is determined by the formula

$$P = F / S_g, \quad F = S_k \tau_{str} \quad (1)$$

where is the force acting from the side of the nozzle on the glue joint of the plug membrane, without taking into account the influx; S_g – the area of the force action corresponding to the area of the inner surface of the nozzle plug membrane; S_k – area of the bonded surface (area of the outer area of the nozzle plug body); τ_{str} – shear stress between the materials of the nozzle and the plug, obtained experimentally (accepted $\tau_{str} = 0,57\sigma_{str}$), σ_{str} – tensile strength with uniform separation.

Taking into account the technical conditions for the use of a nozzle plug made of 3D printing materials, namely that the strength of the adhesive bond of the plug insert must be higher than the response strength of the joint between the body and the plug membrane. The safety factor is chosen 1.5. The plug actuation pressure is $(0,6 \pm 0,3)$ MPa, the calculation uses the maximum value of 0,9 MPa. The inner surface area of the membrane is 222.87 cm². The tensile strength at uniform tearing in the package “carbon fiber material of the socket Ural Tr3 / 2-15 (LBS-20) – epoxy glue EPOTERM-03t type A – material Ultem 9085” was determined experimentally. The average value is $\sigma_{str} = 10.6$ MPa. Thus, we have

$$S_k = k_3 P S_g / 0,57 \sigma_{str},$$

$$S_k = 1,5 \cdot 9 \cdot 222,87 / 0,57 \cdot 108,09 = 48,83 \text{ cm}^2. \quad (2)$$

Based on the calculations performed, the preliminary area of the outer wall of the nozzle plug body was selected, which is 48.83 cm².

Test procedure

Functional tests for actuation were carried out on a special installation with the implementation of a pneumatic pulse into the inner cavity of the plug. The model and photo of the installation are shown in Fig. 6. The principle of operation of the installation is as follows: when the solenoid valve is closed, a pressure is created in the receiver with a value of 5,5 MPa. The length of the pipeline from the receiver to the product, the volume of the test equipment and

the passage of the pipeline are selected so that they are as close as possible to the standard loading conditions. When the valve was opened remotely, a pneumatic pulse was applied to the inner side of the membrane. In this case, the pressure and the response time of the nozzle plug are recorded by a pressure sensor installed in the test equipment. The tests are carried out in three successive stages: checking the tightness of all joints of the tooling and the pneumatic line, confirming the quality of the adhesive of the nozzle plug with the tooling by testing the connection for tightness and, directly, the functional tests themselves.

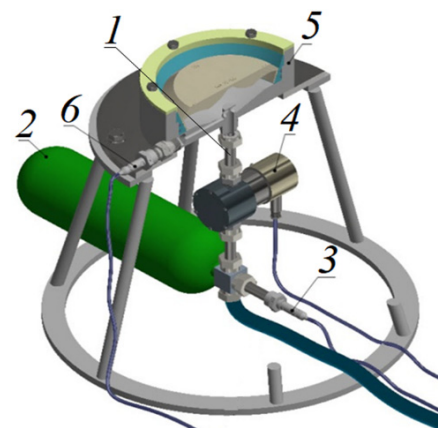


Fig. 6. Model and photo of the installation for functional tests for plug actuation: 1 – pipeline with a nominal bore of 12 mm; 2 – receiver; 3 – pressure sensor; 4 – electromagnetic valve; 5 – test equipment; 6 – pressure sensor

To carry out tests on the study of the permeability of the plugs, special equipment was designed and manufactured (Fig. 7). The test method consists in creating in the inner part of the plug a vacuum of air with a value of more than 100 Pa with fixing the decay of the vacuum for 15 minutes. The test results are considered satisfactory with no drop at all [6].

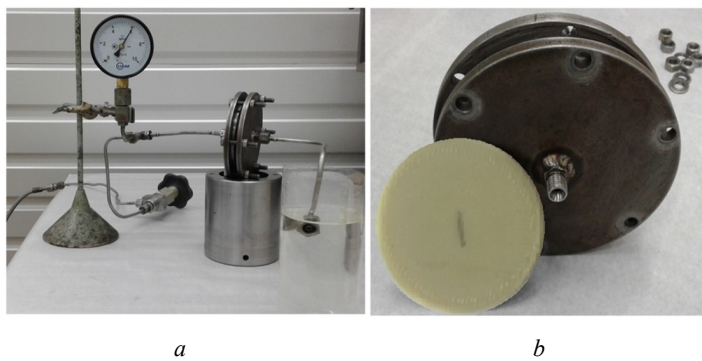


Fig. 7. Stand for testing for permeability (a) and an open fixture with an installed sample (b)

Prior to the tripping tests, an important task was to carry out a gas-dynamic calculation in order to determine the required pressure in the receiver, providing a load simulating the operational one. For this, the flow of a three-dimensional single-phase compressed air flow along the tooling path was simulated. At the inlet to the tract, the pressure in the receiver was set, and at the outlet, the air flow rate, that is, the mass of air in the receiver at a given pressure. The calculation is carried out in a stationary setting, while the pressure from the side of the working cavity of the plug, considering the total pressure loss, should not

be lower than the expected pressure of its operation of the plug, that is 0,6 MPa.

The tests also involved a series of experiments on the triggering of the nozzle plug now of the gas pulse. To implement the destruction process, it is through the glue joint that four designs of plugs with an increased membrane thickness and a double-reinforced joint between the body and the membrane were made in turn. To simulate a standard connection, an engine nozzle simulator was used during pasting.

Changes in the properties of materials used for printing, the lack of information on the degradation of products made from an additive material under the influence of environmental factors, necessitated a series of tests aimed at identifying patterns of decrease in the mechanical properties of the product during storage and operation.

For accelerated climatic tests (ACT), simulating the temperature and humidity effect on the finished product during storage for 12 years, a few successive impacts on materials were carried out:

- ACTs simulating seasonal temperature changes (Table 2);
- ACTs simulating daily temperature and humidity effects (Table 3).

Table 2. ACT modes simulating seasonal temperature changes over 12 years

№	Type of impact	Temperature, °C	Humidity, %	Exposure duration
Tests for seasonal temperature changes				
1	1.1 Exposure at normal temperature	+ (20±5)	Up to 80	4 h
	1.2 Exposure in cold chamber	+ (63±5)	not controlled	4 h
	1.3 Exposure at normal temperature	+ (20±5)	Up to 80	4 h
	1.4 Exposure in cold chamber	– (43±5)	not regulated	4 h
Test on 1.1, 1.2, 1.3, 1.4 alternately 12 times				
2	Exposure at normal temperature	+ (20±5)	Up to 80	4 h

Table 3. ACT modes simulating daily temperature and humidity effects for 12 years

№	Type of impact	Temperature, °C	Humidity, %	Exposure duration
Tests for daily cycle resistance (with transitions through 0 °C)				
3	3.1 Exposure in cold chamber	– 15	not regulated	4 h
	3.2 Exposure at normal temperature	+ (20±5)	up to 80	4 h
Tests according to 3.1, 3.2 of this table should be carried out 10 times in turn				
Heat aging				
4	Heating to heat aging temperature	+ (72±4)	not controlled	4 h
5	Heat aging	+ (72±4)	not controlled	6 day 10h
6	Exposure at normal temperature	+ (20±5)	up to 80	4 h
Tests for moisture resistance with passing through 0 °C				
7	7.1 Exposure in a humidity chamber	+ (25±6)	96–100	20 h
	7.2 Exposure in cold chamber	– 15	not regulated	4 h
Tests according to 7.1, 7.2 of this table should be carried out 10 times in turn				
8	Exposure at normal temperature	+ (20±5)	Up to 80	4 h
Tests according to 3...8 of this table should be carried out 12 times in turn				

Duration of tests with simulation of seasonal changes – 8 days 4 hours. Duration of tests with imitation of daily temperature and humidity effects for one year – 20 days 6 hours, 243 days for 12 years. The total duration of ACT for 12 years of storage will be 251 days 4 hours.

Result and discussion

Result of impregnation was possible to obtain a sufficiently tight surface layer shown in Fig. 8, *a*. Shows typical microstructures for two impregnation methods: Fig. 8, *b* – for impregnation method 1, Fig. 8, *c* – for impregnation method 2. As you can see, in the first case, the glue penetrated into the sample surface to a depth of two to four layers over the entire outer surface sample. In the second case, the glue penetrated to the entire depth, but there are local through cavities along the edges of the sample, which were located at the boundary of the action of vacuum in the tooling under the rubber ring.

Mechanical tests and subsequent fracture analysis of prototype samples showed the following. For sample No. 1, the destruction occurred partially not in the calculated place and between the layers of the print. This can be explained by the fact that the anisotropy of properties was not taken into account when laying out the layers. The destruction of the nozzle plug No. 2 occurred almost at the calculated location, but at the same time, a part of the body with a height of ≈ 25 mm was also torn off. And only sample No. 3 showed the convergence of the calculated and experimental results: during the tests, the destruction of the nozzle plug occurred in the calculated place.

Smooth pressure loading of the test specimens showed quite interesting results. Due to the permeability of the material, the pressure was partially vented, and at low air inflows on the experimental, the destruction of the sample practically did not occur [5].

Penetration tests were carried out initially with plugs prior to impregnation. For the entire batch of nozzle plugs,

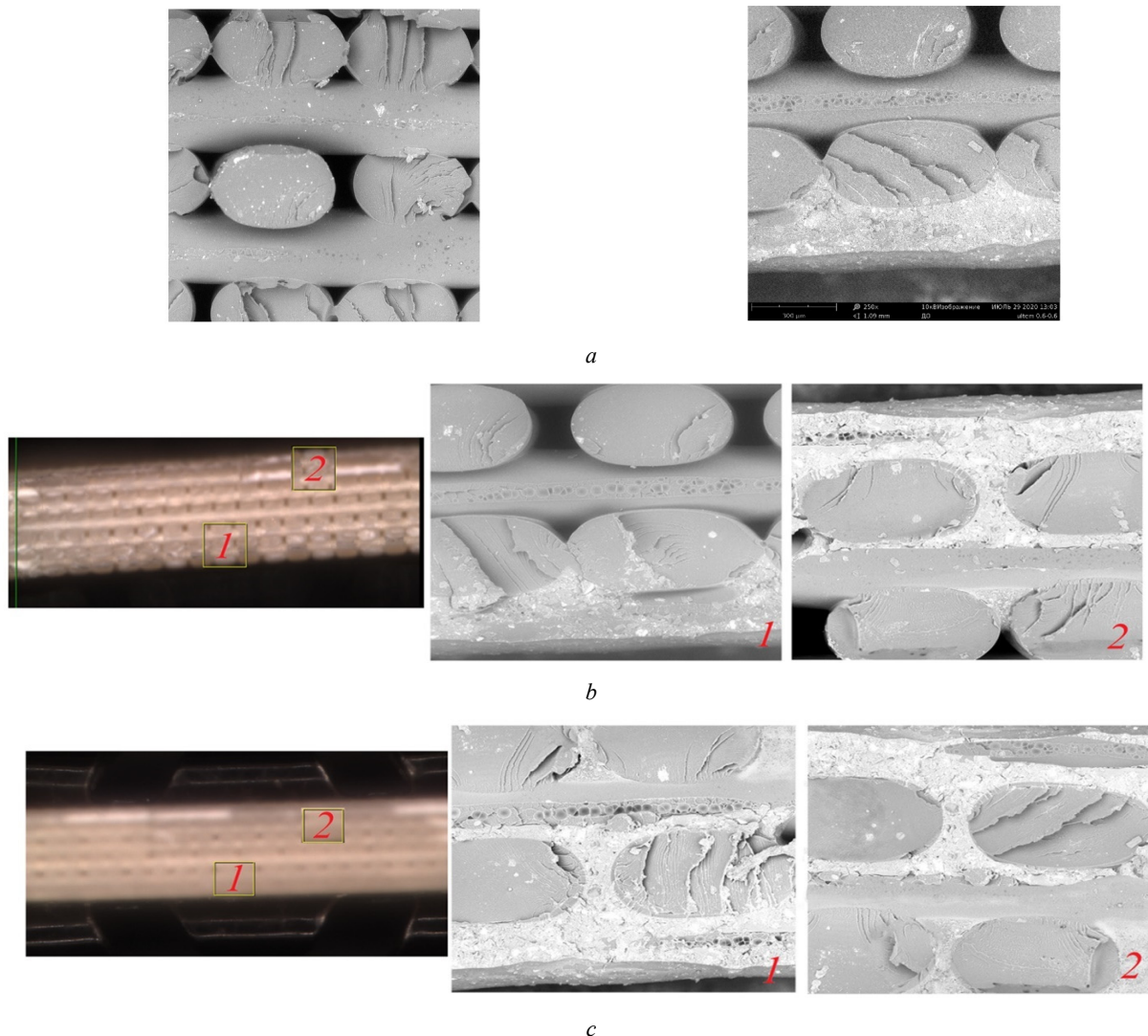


Fig. 8. Microstructure of the sample end after impregnation: *a* – after printing and after impregnation with an adhesive composition; *b* – by method 1 and *c* – by method 2

a complete decay of vacuum discharge was recorded within 15–45 seconds after the valve was closed. During tests, 20 out of 24 plugs after impregnation confirmed their impermeability, for 4 (17% of the batch) plugs a decrease in vacuum discharge was recorded, while the drop was much slower than that of plugs before impregnation.

The time to complete decline was 5–7 minutes. To analyze the reasons for the permeability of the nozzle plug material, a comparison was made of the glue deposition by weighing the parts in different states, because of which it was concluded that all plugs in the batch, including the permeable ones, had the same deposition within the total spread (the average plug mass before impregnation was 297.70 grams, 301.03 grams after impregnation).

The caps were found to be permeable due to individual permeable pores that were not impregnated after the first application cycle. For these plugs, a second impregnation was carried out with an increase in the exposure time during the application of glue to 10 minutes and a cyclic application of glue was introduced. After re-impregnation, the parts proved to be impermeable when tested again. Subsequently, for the second and third batch of nozzle plugs in the amount of 24 pieces, each modified technology made it possible to obtain impermeable nozzle plugs in one impregnation step.

To confirm the correctness of the design and technological solutions incorporated in the design of the nozzle plug, functional tests of operation on 7 plugs were carried out. All tests, regardless of the values, collapsed at a given place, namely in the zone of transition from the body to the nozzle membrane. The first plug was tested with a receiver pressure of 4.875 MPa (calculated). The results of pressure measurements in the cavity of the nozzle plug are shown in Fig. 9.

For comparison, the figure shows the experimental dependence of the pressure in the combustion chamber on time. Obviously, the calculated pressure in the receiver is not enough to simulate the speed of the pneumatic pulse.

For the second nozzle plug, the pressure in the receiver is 5.5 MPa. The measurement results are also shown in the figure. Considering the dependence of the rate of pressure build-up in the combustion chamber, in terms of its angle of inclination to the ordinate axis, to the ratio of the rate of pressure build-up in the cavity of the tooling during functional tests, it can be argued that the pressure value in the receiver cavity is correctly selected ($5.0 \pm 0,5$) MPa, flow sections of the equipment and length of pipelines to simulate the rate of pressure rise in the combustion chamber. The remaining 5 nozzle plugs were tested according to the mode of the second experiment.

The actuation test was carried out on a special installation with the implementation of a pneumatic pulse into the inner cavity of the plug, simulating the standard parameters of the aerodynamic flow when the engine was turned on.

Previous the calculation was carried out in the Ansys CFX package to the level of pressure in chamber determine. The calculation results are shown in Fig. 9. As can be seen from the calculation results, the pressure in the receiver must be at least 4,85 MPa

The mechanism of destruction of plugs is analyzed in detail, considering the implementation of various glue joints.

In the first design of the nozzle plug, the outer side of the body (gluing surface) was made with a calculated area and with a smooth surface. Before pasting, this surface and the nozzles corresponding to it on the simulator were sanded and degreased. Glue was applied to both surfaces in equal proportions, then the positioning of the plug was carried out. During the tests, the destruction of the adhesive joint occurred at a pressure of 0,335 MPa, which is 24.8% of the design pressure of 1,35 MPa, considering the safety factor. An external examination of the plug after triggering (Fig. 10) revealed unsatisfactory cleaning of the glued surfaces and uneven application of glue, there are places where there is no glue. This is also explained by the dif-

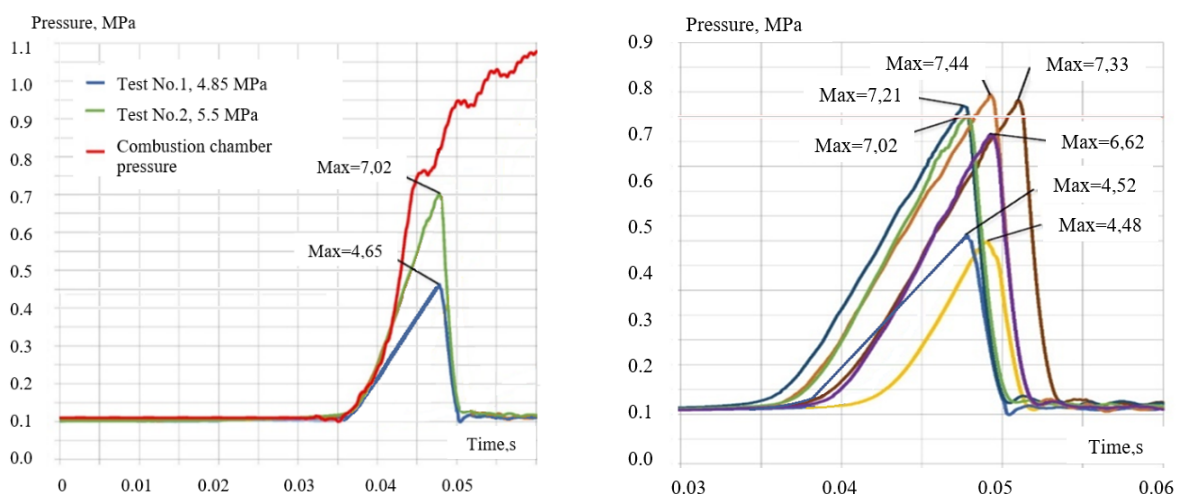


Fig. 9. Results of measurements of pressure in the cavity of the tooling during functional tests

difficulty of positioning the plug relative to the surface of the nozzle, glue flowing out and the inability to uniformly apply pressure to the bonding site during the glue drying. Based on the results of the experiment for the second sample, it was decided to double the gluing area (97.66 cm^2) and to refine the gluing technology by changing the gluing surface.

and complexity in one technological approach without additional mechanical processing. As a result of the tests, the destruction of the adhesive bond occurred at 1,21 MPa, which is 31% higher than the previous one, which indicates the efficiency of using the surface texture. Despite all the modifications of the technological inserts, the obtained value is 0,139 MPa from the required value. For the fourth

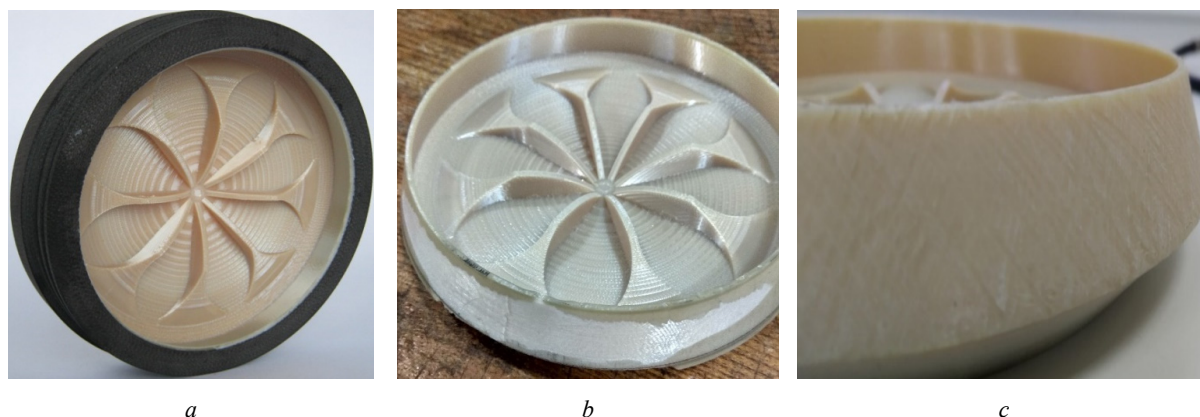


Fig. 10. Sample of plug (a), membrane (b) and layer of glue (c)

In the second case, mechanical cleaning of the bonded surface of the plug was performed with the application of intersecting marks along the entire outer surface of the body to increase the area of the bonded surface (Fig. 9). The amount of glue used has also been increased. During the tests, destruction occurred at 0,923 MPa, which is 2.76 times higher than the first result.

Considering the 2 times increase in the area, the surface treatment technology made it possible to increase the strength by 1.38 times. When examining the plug, similar problems were noted as in the first experiment: when gluing in, the distance from the walls of the plug to the walls of the nozzle simulator is not the same around the circumference, there are distortions, and during installation the glue is squeezed out of the gluing zone.

To obtain a positive result in terms of the work of the glue for the standard connection “carbon fiber-glue-thermoplastic” and to simplify the process of preparing the nozzle plug for gluing, a design change was made (type 3 design) in terms of texture printing over the entire outer surface and protrusions located in three places with a height of 0.3 mm at an angle of 120° along the entire circumference of the body (Fig. 11). The configuration changes increased the surface area of the body by approximately 60 % with a constant glue area, which, combined with the protrusions, allowed the part to be evenly positioned in the nozzle, to ensure a constant glue layer thickness over the entire surface and to reduce glue leakage during installation and drying. The manufacture of such a surface, in contrast to mechanical processing, fully meets the philosophy of manufacturing using the 3D printing method, namely, the manufacture of a product of any shape

and complexity in one technological approach without additional mechanical processing. As a result of the tests, the destruction of the adhesive bond occurred at 1,21 MPa, which is 31% higher than the previous one, which indicates the efficiency of using the surface texture. Despite all the modifications of the technological inserts, the obtained value is 0,139 MPa from the required value. For the fourth

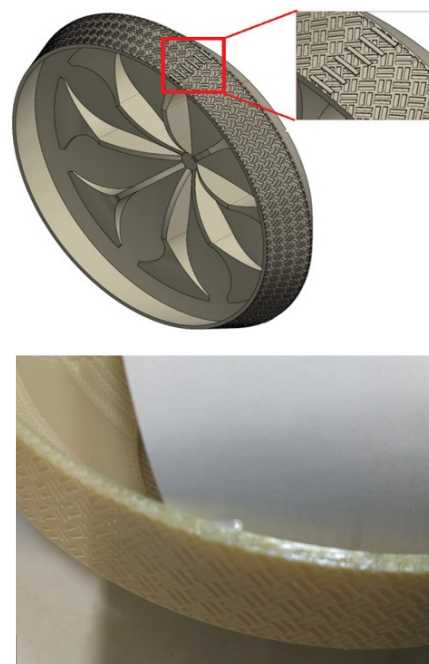


Fig. 11. The plug unit with a texture and tabs for pasting

Thus, the area of the outer surface of the nozzle plug body was 108.8 cm^2 (the increase was 11.14 cm^2). As a result of its tests, the fracture pressure was obtained at 1,370 MPa, which slightly exceeds the required level of 1,35 MPa.

As a result of the work carried out, a reliable adhesive bond of the membrane with the engine working surface was obtained. However, the strength of the adhesive bond in the product is 2.23 times lower than the normative one, which necessitates the search for new methods and techniques of bonding.

Climatic tests showed the following. All samples that were subjected to accelerated climatic tests did not lose the declared mechanical characteristics determined on the basis of test studies before climatic tests.

The test time (which corresponded to the storage time of the products in operation) had almost no effect on the dynamic properties of the opening of the products at the time of starting the engines. Detailing shows next sides. Physical and mechanical tests of the samples showed that PKV affect the characteristics of the material thermoplastic brand ULTEM 9085 as follows: tensile strength - decreases by 4.38 % and 10.99 % for samples printed in the direction of XZ and ZX, respectively; tensile modulus - increases by 3.77 % and 18.05 % for samples printed in the direction XZ and ZX, respectively; elongation at tension - decreases by 7.70 % and 27.30 % for samples printed in the direction XZ and ZX, respectively; compressive strength - increases by 1.94 % and 10.08 % for samples printed in the direction of XZ and ZX, respectively; compression module - decreases by 3.61 % and 5.35 % for samples printed in the direction of XZ and ZX, respectively; flexural strength - increases by 4.86 % for samples printed in the XZ direction and decreases by 6.39 % for samples printed in the ZX direction; modulus at bending – increases by 6.58 % and

12.33 % for samples printed in the direction XZ and ZX, respectively.

From the obtained data it is seen that most of the PKV influenced the characteristics of the samples of ULTEM 9085 thermoplastic material printed in the ZX direction.

Conclusions

As can be seen from the figure, all nozzle plugs during functional tests for actuation comply with the requirement for the actuation pressure range, which is $(0,6 \pm 0,3)$ MPa. As a result of the experiments, the response range was $(0,6 \pm 0,15)$ MPa, which is 2 times less than the specified one. The average response pressure is 0,639 MPa. The average response time is 0.01 s, which in turn corresponds to the experimental pressure in the combustion chamber. Thus, it can be argued that the selected design and applied technologies meet the technical and functional requirements for the nozzle plug.

Thus, we can conclude that the use of ULTEM 9085 material impregnated with EPOTHERM-03t type A epoxy glue makes it possible to obtain high-quality critical elements of RST. The properties of materials were investigated considering their guaranteed shelf life for 12 years of operation under accelerated climatic tests. It is shown that the production of products by FDM-printing methods is promising and expedient, since the properties being formed are predictable, achievable, and stable.

References

- [1] S.H. Konyukhov, “Naukovo-tekhichni napryamy rozrobok kosmichnykh aparativ KB “Pivdenne” im. M. K. Yanhelya”, *Kosmichna nauka i tekhnolohiya*, No. 1, 1995, pp. 12–34. <https://doi.org/10.15407/knit1995.01.012>
- [2] V.N. Hushchyn, *Osnovy prystroyu kosmichnykh aparativ*, Moscow: Mashynobuduvannya, 2003.
- [3] Wu Wenzheng *et al.*, “Influence of Layer Thickness and Raster Angle on the Mechanical Properties of 3D-Printed ULTEM™ 9085 PEI and a Comparative Mechanical Study between PEEK and ABS”, *Materials*, 2015, 8(9), pp. 5834–5846. <https://doi.org/10.3390/ma8095271>
- [4] J.T. Quigley, “Chinese Scientists Are 3D-Printing Ears and Livers – With Living Tissue”, *The Diplomat*, Tech Biz, (Aug. 15, 2013).
- [5] ISO 1701-1:2004. Test conditions for milling machines with table of variable height - Testing of the accuracy. Part 1: Machines with vertical spindle, 2004.
- [6] Official catalog Hiwin [Online]. Available: <https://www.hiwin.com/linear-guideways.html>
- [7] V.V. Pushkarev and A.V. Drobotov, Arrangement of devices for volume printing by extruded molten parts of complex shape, 2016.
- [8] Dynamic extrusion speed. [Online]. Available: <https://3dtoday.ru/questions/dinamicheskaya-skorost-ekstruzii>
- [9] Defects of 3D printing. [Online]. Available: <https://3dtoday.ru/blogs/leoluch/defects-3d-printing-will-try-to-introduce-a-classification>
- [10] A. Salenko *et al.*, “Ensuring the functional properties of responsible structural plastic elements by means of 3-D printing”, *Eastern-European Journal of Enterprise Technologies*, 5/1 (107), 2020. pp.18–28. DOI: 10.15587/1729-4061.2020.211752
- [11] V.V. Bliznichenko, *Proektuvannya i konstruktsiya raket-nosiyiv*, S.M. Konyukhova, Ed., Donetsk: DNU, 2007.
- [12] I. Derevyanko *et al.*, “Eksperimental'nii analiz mekhanichnikh kharakteristik detalei raket-nosiiv, vigotovlenikh za dopomogyu FDM aditivnykh tekhnologii”, *Tekhnichna mekhanika*, No. 1 pp. 92–100, 2021. <https://doi.org/10.15407/itm2021.01.092>
- [13] Standard Test Method for In-Plane Shear Response of Polymer Matrix Composite Materials by Tensile Test of a Composites Laminate, ASTM D3518. ASTM International, 2018.

Создание уплотненных высокопрочных конструкций ракетно-космического оборудования FDM печатью ULTEM™ 9085 PEI пластиком

А.Ф. Саленко, И.И. Деревянко, А.А. Самусенко, К.В. Аврамов, А.В. Литот, В.В. Рогулин

Аннотация. В работе показана возможность изготовления изделий для ракетно-космической техники с использованием аддитивной технологии FDM-печати. Объект исследования – заглушки сопла “мембранного” типа. С учетом удельных прочностных свойств изделия, требуемых при эксплуатации, а также особенностей FDM-процесса, была оптимизирована конструкция, установлены закономерности формирования свойств изделия. Для герметизации изделия была разработана технология пропитки. Спроектировано оборудование и проведены рабочие испытания. Свойства материалов исследованы с учетом гарантированного срока хранения изделия в течение 12 лет эксплуатации в условиях ускоренных климатических испытаний.

Показано, что изготовление изделий методом FDM-печати перспективно и целесообразно, так как формируемые свойства превосходят, достижимы и стабильны.

Ключевые слова: пробка сопла, аддитивные технологии, 3D-печать, прочностные расчеты, пневматические испытания.

Створення ущільнених високоміцних конструкцій ракетно-космічного обладнання FDM друку ULTEM™ 9085 PEI пластиком

О.Ф. Саленко, І.І. Дерев'янку, О.А. Самусенко, К.В. Аврамов, О.В. Литот, В.В. Рогулін

Анотація. У роботі показано можливість виготовлення виробів для ракетно-космічної техніки з використанням адитивної технології FDM-друку. Об'єкт дослідження – заглушки сопла “мембранного” типу. З урахуванням питомих властивостей міцності виробу, необхідних при експлуатації, а також особливостей FDM-процесу, була оптимізована конструкція, встановлені закономірності формування властивостей виробу. Для герметизації виробу була розроблена технологія просочення. Спроектвано обладнання та проведено робочі випробування. Властивості матеріалів досліджено з урахуванням гарантованого терміну зберігання виробу протягом 12 років експлуатації за умов прискорених кліматичних випробувань.

Показано, що виготовлення виробів методами FDM-друку є перспективним і доцільним, оскільки формовані властивості передбачувані, досяжні та стабільні.

Ключові слова: пробка сопла, адитивні технології, 3D-друк, розрахунки на міцність, пневматичні випробування.